ChemComm

RSC Publishing

COMMUNICATION

View Article Online
View Journal | View Issue

Catalytic and regiospecific extradiol cleavage of catechol by a biomimetic iron complex†

Cite this: *Chem. Commun.*, 2013, **49**, 10251

Received 1st June 2013,
Accepted 10th September 2013

DOI: 10.1039/c3cc44124e

www.rsc.org/chemcomm

Sayanti Chatterjee, Debobrata Sheet and Tapan Kanti Paine*

An iron(III)–catecholate complex of a facial tridentate ligand reacts with dioxygen in the presence of ammonium acetate–acetic acid buffer to cleave the aromatic C–C bond of 3,5-di-*tert*-butylcatechol regiospecifically resulting in the formation of an extradiol product with multiple turnovers.

Extradiol catechol dioxygenases oxidatively cleave the C1–C6 bond of catecholate in the biodegradation of aromatic molecules to aliphatic products with incorporation of both atoms of dioxygen into cleavage products.[1] Substrate-bound crystal structures of 2,3-dihydroxybiphenyl 1,2-dioxygenase (BphC), protocatechuate 4,5-dioxygenase (LigAB), and 3,4-dihydroxyphenylacetate 2,3-dioxygenase (2,3-HPCD)[2] have revealed a '2-His-1-carboxylate facial triad motif'[3] at the active site. The mechanism of the extradiol cleavage reaction of catechol has been substantiated by enzymatic, biomimetic and theoretical studies.[4] The oxidative C–C bond cleavage takes place *via* Criegee rearrangement of an iron–peroxo intermediate.[1b] The catalytic activity and selectivity of the enzymatic reaction is controlled not only by the active site but also by the secondary structure of the proteins. Structural and biochemical studies on enzymes revealed a distinct role of the second-sphere residues in the catalytic activities of regiospecific cleavage of catechol.[1a,5] The mutant of catechol dioxygenase from *Escherichia coli*, 2,3-dihydroxyphenylpropionate 1,2-dioxygenase (MhpB) obtained by replacing either His-115 or His-179, lacks extradiol activity, indicating that each of these conserved histidine residues is essential for acid–base catalysis.[5a,b,6] Therefore, control of both first- and second-sphere interactions is necessary to achieve functional models that are expected to display enzyme-like activity.[7] Despite the existence of a large number of iron–catecholate complexes as functional models of extradiol catechol dioxygenases,[8] there is no example of a biomimetic iron complex that exhibits catalytic and specific extradiol cleavage reactivity in the presence of dioxygen.

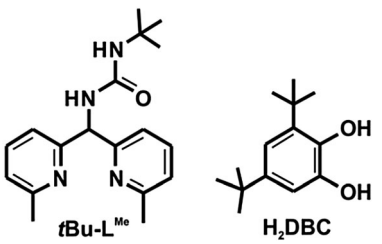

Fig. 1 Ligand and substrate.

As a part of our ongoing research on the development of functional models of nonheme iron oxygenases,[9] we have designed a new urea-based facial tridentate ligand. In this communication, we report the synthesis and characterization of an iron(II)–chloro complex, $[(t\text{Bu-L}^{Me})\text{Fe}^{II}(\text{Cl})_2(\text{MeOH})]$ (**1**), and of an iron(III)–catecholate complex, $[(t\text{Bu-L}^{Me})\text{Fe}^{III}(\text{DBC})](\text{ClO}_4)$ (**2**), where DBC = dianionic 3,5-di-*tert*-butylcatecholate, supported by the facial tridentate ligand, *t*Bu-L^{Me} (Fig. 1). The oxidative C–C bond cleavage of DBC on the iron complexes and their efficiencies as catalytic functional models are discussed. The effect of acid/base on the catalytic and regiospecific extradiol cleavage of catechol is highlighted.

The ligand *t*Bu-L^{Me} was synthesized in good yield from the reaction of bis(6-methylpyridin-2-yl)methanamine with *tert*-butyl isocyanate in dry tetrahydrofuran (Scheme S1, ESI†). The iron(II)–chloro complex (**1**) was prepared by mixing the ligand with $FeCl_2$ in methanol. Complex **2** was isolated from the reaction of ligand, iron(III) perchlorate and 3,5-di-*tert*-butylcatechol (H_2DBC) in the presence of two equivalents of triethylamine in methanol under an inert atmosphere (see experimental, ESI†). The blue solution of complex **2** in acetonitrile displays an intense and broad absorption band at around 600 nm typical of catecholate-to-iron(III) charge-transfer (CT) transition (Fig. S1, ESI†). A similar optical spectrum is obtained when complex **1** is treated with a basic solution of H_2DBC in acetonitrile. The ^{1}H NMR spectrum of **1** shows paramagnetically shifted resonances of the protons (Fig. S2, ESI†). The room temperature magnetic moments of 4.86 μ_B for **1** and 5.98 μ_B for **2** are in excellent agreement with the spin-only values for high-spin

Department of Inorganic Chemistry, Indian Association for the Cultivation of Science, 2A&2B Raja S. C. Mullick Road, Jadavpur, Kolkata-700032, India. E-mail: ictkp@iacs.res.in; Fax: +91-33-2473-2805; Tel: +91-33-2473-4971

† Electronic supplementary information (ESI) available: Detailed experimental procedure, crystal data and figures. CCDC 915749. For ESI and crystallographic data in CIF or other electronic format see DOI: 10.1039/c3cc44124e

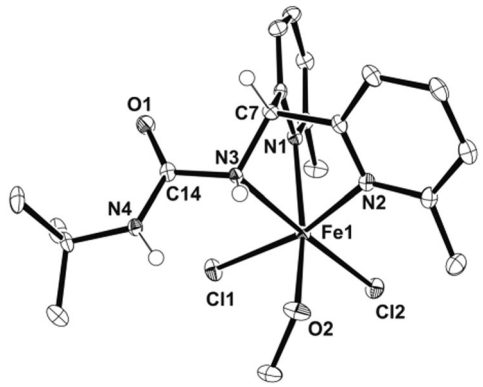

Fig. 2 ORTEP plot of complex **1** with 40% thermal elliposid parameters. All hydrogen atoms except those on C7, N3 and N4 have been omitted for clarity. Selected bond lengths [Å] and angles [°] for **1**: Fe(1)–N(1) 2.237(2), Fe(1)–N(2) 2.336(2), Fe(1)–N(3) 2.345(3), Fe(1)–O(2) 2.1410(19), Fe(1)–Cl(1) 2.5063(7), Fe(1)–Cl(2) 2.3640(7), N(1)–Fe(1)–N(3) 74.50(8), N(1)–Fe(1)–N(2) 84.12(8), N(1)–Fe(1)–O(2) 158.56(9), N(2)–Fe(1)–O(2) 83.62(7), N(3)–Fe(1)–O(2) 84.75(8), Cl(1)–Fe(1)–Cl(2) 93.09(3), Cl(1)–Fe(1)–N(1) 92.00(6), Cl(1)–Fe(1)–N(2) 162.51(6), Cl(2)–Fe(1)–N(3) 173.35(6).

iron(II) and iron(III) complexes, respectively. The X-band EPR spectrum of **2** at 77 K exhibits a rhombic signal at $g = 4.2$ typical of high-spin iron(III) complexes (Fig. S3, ESI†).

The X-ray crystal structure of the neutral complex (**1**) reveals a six-coordinate distorted octahedral coordination geometry at the iron center (Fig. 2). The tridentate ligand occupies one face of the octahedron through two pyridine nitrogens (N1 and N2) and the nitrogen atom N3 of the urea moiety. The other face is occupied by two chloride ions and a solvent methanol molecule. Two pyridine nitrogens (N1 and N2), one chloride atom (Cl1) and the oxygen atom (O2) of a methanol molecule occupy the equatorial plane. The urea nitrogen (N3) and the other chloride donor (Cl2) occupy the axial positions with the Cl2–Fe1–N3 angle of 173.35(6)°. The metal–ligand bond distances are typical of a high-spin iron(II) complex (Table S1, ESI†). The average iron–nitrogen distance (2.30 Å) is found to be unusually longer. Such a long iron–nitrogen bond has been observed in the ($^{t\mathrm{Bu}}$PNP)FeCl$_2$ complex of a PNP-pincer ligand ($^{t\mathrm{Bu}}$PNP = 2,6-bis(di-*tert*-butylphosphinomethyl)-pyridine).[10] All attempts to isolate the single crystal of the iron(III)–catecholate complex (**2**) were unsuccessful.

The iron(III)–catecholate complex **2** reacts with dioxygen in acetonitrile during which the CT band at around 600 nm slowly decays and the blue solution turns light green over a period of 5 h (Fig. S4, ESI†). The ^{1}H NMR spectrum of the organic product reveals only 25% conversion of catechol to an extradiol cleavage product, 4,6-di-*tert*-butyl-2-pyrone (Fig. S5, ESI†). Labelling experiment with $^{18}O_2$ supports the incorporation of one oxygen atom from dioxygen into the cleavage product (Fig. S6, ESI†). Complex **1**, otherwise unreactive towards O_2, reacts with H_2DBC in the presence of dioxygen to afford almost the same amount of the extradiol product. The analysis of the catechol-cleavage product in the presence of different protic acids like acetic acid ($pK_a = 4.74$), pyridinium perchlorate ($pK_a = 5.25$) and piperidinium perchlorate ($pK_a = 11.29$) indicates that pyridinium perchlorate is the best acid (Fig. S7, ESI†). The amount of pyridinium perchlorate also has an effect on the yield of the catechol cleavage product (Fig. S8, ESI†). Complex **2** affords 95% extradiol product in the presence of one equivalent of pyridinium perchlorate. Acid plays a crucial role in controlling the regiospecific C–C bond cleavage of H_2DBC, and an optimum pK_a value brings out the best yield of the extradiol cleavage product.

Interestingly, complex **2** reacts with oxygen at room temperature in a mixture of MeCN and NH_4OAc–AcOH buffer (4 : 1) during which the catecholate-to-Fe(III) CT band decays much faster ($k_{obs} = 3.86 \times 10^{-3}$ s^{-1}) compared to normal decay or decay in the presence of protic acid only. A ten-fold increase in the reaction rate is observed (Fig. S9, ESI†). Analyses of the organic product after the reaction clearly suggest the formation of 94–95% extradiol cleavage product within 40 min. The final solution of **2** reacts further with excess H_2DBC at pH = 5.5 to regenerate the characteristic CT band. Moreover, complex **2** was found to be stable in the presence of 100 fold excess of H_2DBC at pH = 5.5. These intriguing results prompted us to study the catalytic activity of **2** in MeCN–NH_4OAc–AcOH buffer. With increasing amounts of catechol the turnover number (TON) is increased giving rise to 4,6-di-*tert*-butyl-2-pyrone as the only product (Scheme 1 and Fig. S10, ESI†). A maximum TON of 34 at pH = 5.5 after 8 h is observed with 100 equiv. of H_2DBC (Fig. S11, ESI†). When complex **1** is used as a catalyst under the same experimental conditions, a maximum TON of 33 is observed. The catalytic results obtained with complex **1** support the *in situ* formation of **2** during the reaction. The catalytic activities of iron complexes not only depend on the concentration of the substrate, but are also affected by the pH of the reaction medium. The use of buffer with higher or lower pH exhibits a lower catalytic TON (Fig. 3). After 8 h, the pH of the reaction solution increases above 6 possibly due to hydrolysis of the urea ligand and as a result no change in TON is observed (Fig. S12, ESI†). Of note, the native enzyme MhpB exhibits a k_{cat} value of 29 s^{-1} on the basis of the catalytic ability per 80 kDa subunit.[5b]

In biomimetic chemistry, only a few model complexes are known which catalytically oxidize H_2DBC with molecular oxygen.[11] These model complexes however exhibit low selectivity towards extradiol cleavage. An efficient and catalytically active functional model, [(L-N_4Me_2)Fe(dbc)]$^+$ (L-N_4Me_2 = *N*,*N*′-dimethyl-2,11-diaza-[3.3](2,6)pyridinophane), of intradiol cleaving dioxygenases has

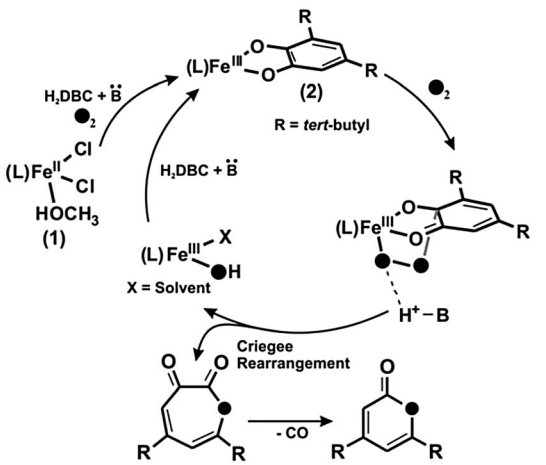

Scheme 1 Proposed catalytic pathway for regiospecific C–C bond cleavage of catechol in the presence of molecular dioxygen.

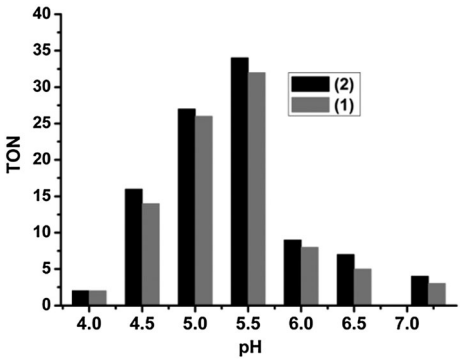

Fig. 3 Dependence of pH on the catalytic TON of extradiol products with **1** and **2**.

been reported.[12] The catalytic and regiospecific extradiol product obtained with the complexes reported here represent the first examples of catalytically active functional models of extradiol-cleaving catechol dioxygenases.

Studies with enzymes and models have established that both iron(II) and iron(III) can catalyze the extradiol cleavage of catechol.[1b,5a,8c] The catalytic extradiol reactivity shown by the iron(III)–catecholate (**2**) and also by the iron(II)–chloro complex (**1**) supports that the catalytic cycle proceeds through an iron(III) complex. The catalytic mechanism shown in Scheme 1, therefore, is not valid for the catalytic cycle of the enzyme. The redox isomer of **2**, an iron(II)-*o*-benzosemiquinonato radical species, reacts with O_2 to form an iron(III)–peroxo intermediate (Scheme 1). The facial coordination of the supporting ligand allows the peroxo intermediate to adopt a pseudo-axial arrangement. The heterolytic O–O bond cleavage involved in Criegee rearrangement is assisted by the presence of a proton affording the extradiol cleavage product.[1b,4e] It is important to mention here that a reported iron(III)–catecholate model complex [(TACN)Fe^{III}(DBC)(Cl)] (**3**) (TACN=1,4,7-triazacyclononane),[8d] which exhibits regioselective (98%) extradiol products, does not exhibit catalytic extradiol cleavage under our experimental conditions (Fig. S13 and S14, ESI†). In the reaction, quinone is formed catalytically with negligible formation of extradiol products (Table S2, ESI†). Therefore, the presence of urea ligand and use of a buffer play crucial roles in directing the regiospecific extradiol cleavage reaction of **1** and **2**. The urea group of the supporting ligand is expected to interact with the iron–peroxo species thereby facilitating the heterolytic O–O bond cleavage towards the extradiol product. The presence of NH_4OAc–AcOH buffer with a pH of 5.5 provides protons required for C–C bond cleavage of catechol and also deprotonates the excess catechol to coordinate to the metal center making the system catalytic.

In conclusion we have prepared and characterized two iron complexes supported by a urea-derived facial tridentate ligand. The iron–catecholate complex is reactive towards dioxygen and specifically cleaves the C–C bond adjacent to the phenolic OH group of 3,5-di-*tert*-butylcatechol mimicking the function of extradiol-cleaving catechol dioxygenases. Proton has a dramatic effect in controlling the regiospecific C–C bond cleavage of catechol on the model complex. The C–C bond cleavage reaction rate increases many fold in the presence of a buffer and the system exhibits catalytic reactivity. Detailed experimental and theoretical studies to get insight into the role of the urea moiety in the regiospecific catechol cleavage pathway are in progress.

TKP acknowledges the Indian National Science Academy (Project for INSA Young Scientist Awardee) for financial support. SC and DS thank CSIR, India, for fellowships. Single Crystal X-ray diffraction data were collected at the Department of Inorganic Chemistry, IACS.

Notes and references

1 (*a*) M. Costas, M. P. Mehn, M. P. Jensen and L. Que, Jr., *Chem. Rev.*, 2004, **104**, 939; (*b*) T. D. H. Bugg and G. Lin, *Chem. Commun.*, 2001, 941; (*c*) F. H. Vaillancourt, J. T. Bolin and L. D. Eltis, *Crit. Rev. Biochem. Mol. Biol.*, 2006, **41**, 241; (*d*) T. D. H. Bugg, *Tetrahedron*, 2003, **59**, 7075.

2 (*a*) S. Han, L. D. Eltis, K. N. Timmis, S. W. Muchmore and J. T. Bolin, *Science*, 1995, **270**, 976; (*b*) A. Kita, S. Kita, I. Fujisawa, K. Inaka, T. Ishida, K. Horiike, M. Nozaki and K. Miki, *Structure*, 1999, **7**, 25; (*c*) K. Sugimoto, T. Senda, H. Aoshima, E. Masai, M. Fukuda and Y. Mitsui, *Structure*, 1999, **7**, 953; (*d*) G. P. Titus, H. A. Mueller, J. Burgner, S. R. de Córdoba, M. A. Peñalva and D. E. Timm, *Nat. Struct. Biol.*, 2000, **7**, 542.

3 E. L. Hegg and L. Que, Jr., *Eur. J. Biochem.*, 1997, **250**, 625.

4 (*a*) T. D. H. Bugg and C. J. Winfield, *Nat. Prod. Rep.*, 1998, **15**, 513; (*b*) T. D. H. Bugg and S. Ramaswamy, *Curr. Opin. Chem. Biol.*, 2008, **12**, 134; (*c*) J. D. Lipscomb, *Curr. Opin. Struct. Biol.*, 2008, **18**, 644; (*d*) E. G. Kovaleva and J. D. Lipscomb, *Science*, 2007, **316**, 453; (*e*) R. J. Deeth and T. D. H. Bugg, *JBIC, J. Biol. Inorg. Chem.*, 2003, **8**, 409; (*f*) P. E. M. Siegbahn and F. Haeffner, *J. Am. Chem. Soc.*, 2004, **126**, 8919; (*g*) M. Y. M. Pau, M. I. Davis, A. M. Orville, J. D. Lipscomb and E. I. Solomon, *J. Am. Chem. Soc.*, 2007, **129**, 1944; (*h*) P. Comba, H. Wadepohl and S. Wunderlich, *Eur. J. Inorg. Chem.*, 2011, 5242; (*i*) G. J. Christian, S. Ye and F. Neese, *Chem. Sci.*, 2012, **3**, 1600.

5 (*a*) S. L. Groce and J. D. Lipscomb, *J. Am. Chem. Soc.*, 2003, **125**, 11780; (*b*) S. Mendel, A. Arndt and T. D. H. Bugg, *Biochemistry*, 2004, **43**, 13390; (*c*) A. J. Fielding, J. D. Lipscomb and L. Que, Jr., *J. Am. Chem. Soc.*, 2012, **134**, 796.

6 M. Brivio, J. Schlosrich, M. Ahmad, C. Tolond and T. D. H. Bugg, *Org. Biomol. Chem.*, 2009, **7**, 1368.

7 R. L. Shook and A. S. Borovik, *Inorg. Chem.*, 2010, **49**, 3646.

8 (*a*) P. C. A. Bruijnincx, M. Lutz, A. L. Spek, W. R. Hagen, B. M. Weckhuysen, G. van Koten and R. J. M. K. Gebbink, *J. Am. Chem. Soc.*, 2007, **129**, 2275; (*b*) S. Paria, P. Halder and T. K. Paine, *Inorg. Chem.*, 2010, **49**, 4518; (*c*) G. Lin, G. Reid and T. D. H. Bugg, *J. Am. Chem. Soc.*, 2001, **123**, 5030; (*d*) M. Ito and L. Que, Jr., *Angew. Chem., Int. Ed.*, 1997, **36**, 1342; (*e*) D.-H. Jo and L. Que, Jr., *Angew. Chem., Int. Ed.*, 2000, **39**, 4284; (*f*) T. Ogihara, S. Hikichi, M. Akita and Y. Moro-oka, *Inorg. Chem.*, 1998, **37**, 2614; (*g*) S. Paria, P. Halder, B. Chakraborty and T. K. Paine, *Indian J. Chem.*, 2011, **50A**, 420.

9 (*a*) T. K. Paine, S. Paria and L. Que, Jr., *Chem. Commun.*, 2010, **46**, 1830; (*b*) S. Paria, L. Que, Jr. and T. K. Paine, *Angew. Chem., Int. Ed.*, 2011, **50**, 11129; (*c*) S. Paria, P. Halder and T. K. Paine, *Angew. Chem., Int. Ed.*, 2012, **51**, 6195; (*d*) O. Das, S. Chatterjee and T. K. Paine, *JBIC, J. Biol. Inorg. Chem.*, 2013, **18**, 401; (*e*) B. Chakraborty and T. K. Paine, *Angew. Chem., Int. Ed.*, 2013, **52**, 920; (*f*) P. Halder, S. Paria and T. K. Paine, *Chem.–Eur. J.*, 2012, **18**, 11778.

10 E. M. Pelczar, T. J. Emge, K. Krogh-Jespersen and A. S. Goldman, *Organometallics*, 2008, **27**, 5759.

11 (*a*) M. G. Weller and U. Weser, *J. Am. Chem. Soc.*, 1982, **104**, 3752; (*b*) T. Funabiki, H. Sakamoto, S. Yoshida and K. Tarama, *J. Chem. Soc., Chem. Commun.*, 1979, 754; (*c*) T. Funabiki, A. Mizoguchi, T. Sugimoto and S. Yoshida, *Chem. Lett.*, 1983, 917; (*d*) M. Duda, M. Pascaly and B. Krebs, *J. Chem. Soc., Chem. Commun.*, 1997, 835; (*e*) T. Funabiki, T. Yamazaki, A. Fukui, T. Tanaka and S. Yoshida, *Angew. Chem., Int. Ed.*, 1998, **37**, 513; (*f*) T. Funabiki, D. Sugio, N. Inui, M. Maeda and Y. Hitomi, *Chem. Commun.*, 2002, 412; (*g*) M. Merkel, D. Schnieders, S. M. Baldeau and B. Krebs, *Eur. J. Inorg. Chem.*, 2004, 783; (*h*) M. Pascaly, M. Duda, F. Schweppe, K. Zurlinden, F. K. Müller and B. Krebs, *J. Chem. Soc., Dalton Trans.*, 2001, 828; (*i*) M. U. Triller, D. Pursche, W.-Y. Hsieh, V. L. Pecoraro, A. Rompel and B. Krebs, *Inorg. Chem.*, 2003, **42**, 6274.

12 W. O. Koch and H.-J. Krüger, *Angew. Chem., Int. Ed.*, 1995, **34**, 2671.